Anal Bioanal Chem
DOI 10.1007/s00216-010-4634-3

ORIGINAL PAPER

Using nanoelectrospray ion mobility spectrometry (GEMMA) to determine the size and relative molecular mass of proteins and protein assemblies: a comparison with MALLS and QELS

E. A. Kapellios · S. Karamanou · M. F. Sardis · M. Aivaliotis · A. Economou · S. A. Pergantis

Received: 9 November 2010 / Revised: 17 December 2010 / Accepted: 20 December 2010

Abstract The determination of protein assembly size and relative molecular mass is currently of great importance in biochemical analysis. In particular, the technique of nanoelectrospray (nES) with a gas-phase electrophoretic mobility molecular analyzer (GEMMA) has received increased attention for such measurements. However, in order for the GEMMA technique to gain broader acceptance in protein analysis, it must be further evaluated and compared with other established bioanalytical techniques. In the present study, nES-GEMMA was evaluated for the analysis of a set of protein and protein complexes involved in the Sec and the bacterial type III secretion pathway of enteropathogenic *Escherichia coli* bacteria. The same set of proteins, isolated and purified using standard biochemical protocols, were also analyzed using multi-angle laser light scattering (MALLS) and quasi-elastic light scattering (QELS), following size exclusion chromatography. This allowed for direct comparisons between the three techniques. It was found that nES-GEMMA, in comparison to the more established MALLS and QELS techniques, offers several complementary advantages. It requires considerably less amount of material, i.e., nanogram vs. milligram amounts, and time per sample analysis, i.e., few minutes vs. tens of minutes. Whereas the determined size and relative molecular mass are similar between the compared methods, the electrophoretic diameters determined using nES-GEMMA seem to be systematically smaller compared to the hydrodynamic diameter derived by QELS. Some of the GEMMA technique disadvantages include its narrow dynamic range, limited by the fact that at elevated protein concentrations there is increased potential for the occurrence of nES-induced oligomers. Thus, it is preferred to analyze dilute protein solutions because non-specific oligomers are less likely to occur whereas biospecific oligomers remain detected. To further understand the formation of nES-oligomers, the effect of buffer concentration on their formation was evaluated. Also, nES-GEMMA is not compatible with all the buffers commonly used with MALLS and QELS. Overall, however, the nES-GEMMA technique shows promise as a high-throughput proteomics/protein structure tool.

Keywords Bioanalytical methods · Mass spectrometry/ICP-MS · Aerosols/particulates

Electronic supplementary material The online version of this article (doi:10.1007/s00216-010-4634-3) contains supplementary material, which is available to authorized users.

E. A. Kapellios · S. A. Pergantis (✉)
Environmental Chemical Processes Laboratory,
Department of Chemistry, University of Crete,
Voutes Campus,
71003 Heraklion, Crete, Greece
e-mail: spergantis@chemistry.uoc.gr

S. Karamanou · M. F. Sardis · M. Aivaliotis · A. Economou (✉)
IMBB-FORTH,
Vassilika Vouton,
71110 Heraklion, Crete, Greece
e-mail: aeconomo@imbb.forth.gr

M. F. Sardis · A. Economou
Department of Biology, University of Crete,
Voutes Campus,
71003 Heraklion, Crete, Greece

Published online: 14 January 2011

Introduction

Protein assemblies play an important role in numerous biological processes, including protein synthesis, folding and trafficking, gene expression, immune recognition, signal transduction, cell motility, and enzymatic reactions [1–3]. As a result, the structural characterization of such native protein states is of paramount importance in biological and biochemical studies. In particular, the stoichiometry and relative molecular mass (M_r) of the native protein complexes are some of the properties that require determining. However, because protein assemblies are usually held together by non-covalent interactions between protein subunits, their analysis requires the use of specialized bioanalytical techniques capable of maintaining native conditions that preserve such non-covalent interactions.

Recently, nanoelectrospray (nES) coupled to either mass spectrometry (MS) or ion mobility spectrometry (IMS) has been shown to be a powerful tool for the structural analysis of protein molecules and assemblies [4–7]. Even though it is an inherently gas-phase technique, nES has been demonstrated to maintain weakly bound non-covalent protein complexes, thus allowing for the detection of intact oligomeric assemblies. This has made nES in combination with MS or IMS eminently suitable for determining the stoichiometry of binding partners in biological complexes [7–11]. One particular combination of nES with IMS, referred to as a gas-phase electrophoretic mobility molecular analyzer (GEMMA), has shown great potential for such measurements [4–6, 12–14]. The critical features of this technique include the conversion of nES-generated multiply charged molecules to their singly charged counterparts by using a bipolar neutralizer [15]. During the charge reduction process, most of the nES-generated gas-phase molecules are neutralized, whereas only a small population possesses a single charge [15–17]. The singly charged macromolecules and their complexes are subsequently separated and "sized" using a differential mobility analyzer (DMA) type ion mobility spectrometer. Macromolecule separation is based on their gas-phase electrophoretic mobility which is a function of their electrophoretic mobility diameter (EMD or D_p) [6]. EMD is defined as the diameter of a singly charged sphere with the same electrophoretic mobility (Z_p) as the analyzed protein. It is this sizing capability that is the distinguishing feature between nES-GEMMA and nES-MS, when the latter is used without ion mobility separation. Also, in nES-GEMMA, the EMD measurements are used to calculate the biomolecule's M_r, as opposed to it being determined from the m/z values of multiply charged biomolecules generated and determined using nES-MS. For the nES-GEMMA measurement of primarily globular proteins, a correlation between EMD and M_r for proteins and protein complexes ranging from 8 kDa to 2 MDa and measuring 2.6–21.7 nm in EMD has been shown [4]. Charged particle detection in nES-GEMMA is usually conducted using a condensation particle counter (CPC) [18, 19], although recently additional modes of online and off-line detection have been developed [13, 20].

Ever since the introduction of the nES-GEMMA technique by Kaufman et al. [6] and its subsequent commercialization, it has been used for various applications involving the determination of the size and M_r of proteins and of other macromolecules, including intact biospecific protein complexes [4, 21–23], viruses [4, 21], virus–antibody complexes [14], virus receptor [14], bacteriophages [24, 25], as well as synthetic polymers [26, 27]. However, the majority of proteins analyzed so far have been commercially available, with few exceptions [4, 13, 23]. Thus, most studies have provided limited information regarding the technique's requirements with respect to sample preparation, as well as its overall capability to handle biological samples prepared in-house using routine biochemical isolation and purification techniques. Further evaluation of nES-GEMMA as a structural elucidation tool for the analysis of biological systems has revealed that measured EMD for selected viruses falls within 15% of the diameters measured by X-ray crystallography [21]. For the major vault proteins (MVP), nES-GEMMA has been used to determine the incorporation of other proteins into their interior after the formation of an MVP-only outer shell [28]. However, it has become evident that in order to advance the applicability of this technique to study large protein complexes, it is critical that the gas-phase characteristics of several additional protein complexes, of varying sizes and shapes (including non-spherical), are examined.

The objectives of the present study include evaluating nES-GEMMA as a structural elucidation tool for studying proteins and protein complexes isolated in-house from the Sec and the bacterial type III secretion pathway of enteropathogenic *Escherichia coli* bacteria. The majority of proteins analyzed were isolated and purified using standard biochemical protocols, developed for use with established bioanalytical techniques such as multi-angle laser light scattering (MALLS) and quasi-elastic light scattering (QELS). In this study, we provide detailed protein measurements using all three techniques, i.e., nES-GEMMA, MALLS, and QELS. Because the same protein samples are analyzed using each of the three techniques, direct comparisons are possible and expected to be of increased validity as protein sample variations are absent or negligible. This comparison between nES-GEMMA and the established MALLS/QELS approaches allows for the identification of the former technique's strengths and limitations, thus allowing for future research that will potentially improve it. Of particular interest, however, is to evaluate the capability of nES-

GEMMA to be used to accurately analyze protein complexes. Because nES-GEMMA is a gas-phase technique, it remains to be clarified whether, and to what extent, its protein and protein complex measurements reflect structural features of their aqueous-phase counterparts. Essentially, this requires understanding a protein molecule's or complex's physical transition from the aqueous phase to the gas phase. The measurements made here contribute toward our further understanding of such physical processes.

Experimental

Materials

Proteins

Several proteins were produced as oligohistidine derivatives and were isolated and purified using established protocols for nickel affinity chromatography [29, 30]. These were: the SecA ATPase and the SecB chaperone of the bacterial protein export system [31], glucose binding protein (GBP) [32], yellow fluorescent protein (YFP) [33], a GBP–YFP hybrid (GBP–YFP), a cyan fluorescent protein–GBP–YFP chimera (CFP–GBP–YFP) [30] (Koukaki et al., in preparation), prolyl isomerase (PPiAase) [34], and the dimeric CesAB chaperone alone or as a complex with its secretory substrate EspA [35]. The latter two proteins were synthesized in an *E. coli* cell, CesAB with an oligohistidine tag for affinity purification and EspA without one. CesAB–EspA complexes were co-purified by metal affinity purification. GBP was prepared to serve as an internal covalent dimer control. For this purpose, a cysteinyl residue was introduced at position 13 of its primary sequence so that the protein forms a disulfide cross-link. The SecA protein was introduced in two versions, SecA 6-901 and Sec 6-834, the latter without its carboxy-terminal tail of 70 residues, which corresponds to a relative mass of approximately 9.7 kDa [31, 36]. For a detailed description of these proteins and their FASTA sequences, see Electronic supplementary material (ESM) Table S1. Proteins (1–20 mg mL^{-1}) were stored at −80 °C in 50 mM Tris–Cl, pH 8.0, supplemented with 50% glycerol. For analysis using nES-GEMMA, they were dialyzed overnight in a 20 mM ammonium acetate (AmAc) buffer and then diluted to various concentrations in 20 mM AmAc immediately prior to their nanoflow infusion into the instrument.

Reagents

Ammonium acetate (puriss. p.a, Reag. ACS) was purchased from Sigma-Aldrich and prepared to various concentrations (20–80 mM). For nES-GEMMA analysis, nanopure water (18.2 $M\Omega^{-1}$ cm^{-1}) produced from a purelab ultra apparatus (Siemens Water Technologies) was used.

Instrumentation and procedure

A nES-GEMMA instrument with a CPC detector from TSI Inc. (St. Paul, MN, USA) was used in this study. The instrument configuration consisted of a nES source unit (model 3480C) equipped with a neutralizing chamber (^{210}Po α-source; 5 mCi, model P-2042 Nucleospot local air ionizer; NRD, Grand Island, NY, USA), whereas the ion mobility spectrometer used for the GEMMA separation was a differential mobility analyzer (TSI Inc., macroIMS, series 3080C). Detection was achieved using a butanol-based Ultrafine CPC (TSI Inc., series 3025A). IMS version 2.0.1.0 (TSI Inc.) software was used for data acquisition and data analysis.

Sample solutions in Eppendorf tubes were placed into the nES unit. One end of a 25-cm-long, 25-μm i.d. (150-μm o.d.) polyimide-coated fused silica capillary was immersed into the solution, while the other end having a conical shape was located within the nES chamber. The spray was achieved by introducing the sample into the capillary by applying air pressure of 3.7 bar and a voltage between +1.5 and +2.5 kV to the Pt wire dipped in the sample solution. This resulted in a nES flow rate of ≈70 nL min^{-1}.

First principles are used to determine the electrophoretic mobility of a nanoparticle as it travels through the ion mobility drift cell (see ESM for relevant equations). This requires knowledge of gas flow rates and drift cell dimensions which are provided by the manufacturer and used automatically by the instrument software. However, the time it takes for the nanoparticle to be counted by the CPC detector after it exits the ion mobility drift cell is determined by calibration. The calibration procedure requires the use of a commercially available protein mixture (High Molecular Weight Calibration Kit for Native Electrophoresis, Amersham, GE Healthcare, UK) which contains bovine serum albumin (M_r=66 kDa), bovine heart lactate dehydrogenase (M_r=140 kDa), bovine liver catalase (M_r=232 kDa), equin spleen ferritin (M_r=440 kDa), and porcine thyroid thyroglobulin (M_r=669 kDa). Technical details of the calibration procedure are described in a Technical Note provided by TSI Inc.

Laser light scattering

Laser light scattering measurements were carried out online following size exclusion chromatography (SEC) using a Shimadzu LC10A-VP HPLC system. SEC was carried out using a prepacked column (Superdex HR200 10/300 GL;

GE) coupled online with four detectors: a photodiode-array detector (SPD-M10AVP; Shimadzu) for UV monitoring at 280 nm; a MALLS detector (DAWN-EOS, Wyatt) using a K5-type cell and a laser wavelength of 690 nm; a QELS detector (WyattQELS; Wyatt) that was connected through an optical fiber to one of the detectors of the MALLS instrument; and a refractive index detector (RID-10A; Shimadzu). MALLS and QELS data were analyzed and plotted using the Astra v.5.0 software (Wyatt). Proteins (5–30 μM in 100- to 150-μL injection volumes) in 50 mM Tris–HCl, pH 8.0, 50 mM KCl, were loaded onto the SEC column and chromatographed at 25 °C at a flow rate of 0.8 mL min^{-1}. However, it should also be mentioned that identical results are obtained when using the ammonium acetate buffer with MALLS/QELS, as demonstrated from the analysis of several of the present study's protein samples (data not shown). The significantly larger number of protein samples analyzed using the Tris buffer allowed for improved statistical analysis, and thus, only the values obtained using this buffer are included and further discussed here.

Results and discussion

nES-GEMMA for protein analysis

In order to illustrate some of the important features of our study, we first discuss the analysis of the well-characterized protein SecA that forms a non-covalent dimer in solution ([31] and references therein). NanoES-GEMMA electropherograms obtained for SecA at two different concentration levels, i.e., 10 and 80 μg protein per milliliter, are shown in Fig. 1. The most intense peak (D^{+1}), observed at an EMD of 10.2 nm, corresponds to a singly charged non-covalent SecA dimer complex (di-SecA). The less intense peaks observed at 7.3, 6.0, and 5.1 nm correspond to doubly, triply, and quadruply charged di-SecA, respectively. The presence of such multi-charged species is attributed to the reduced activity exhibited by the 2-year-old ^{210}Po radioactive α-emitter used for charge reduction in the nES source, whereas a fully active 5-mCi charge reducer does not typically allow for multiply charged nanoparticles. In the present study, the multiply charged species were used to confirm the sizing measurements, as has been reported previously for measurements of synthetic polymers [27].

Comparison of nES-GEMMA with MALLS/QELS for protein analysis

For five replicate nES-GEMMA analyses of the SecA protein sample, the average EMD of the observed di-SecA complex was determined to be 10.08±0.04 nm. This value, along with the M_r calculated from it, were compared with data obtained using two established bioanalytical techniques, i.e., MALLS and QELS, which make measurements in aqueous environment (Table 1). In the case of QELS, a hydrodynamic radius of 5.5 nm was derived, thus corresponding to a hydrodynamic diameter (D_H) of 11.0 nm. The 8.4% size difference observed between the two techniques is in good agreement with the size change expected for the protein aqueous–gas phase transition (≈10% contraction) [37]. Wyttenbach and Bowers [37] have suggested that proteins in the gas phase, under vacuum conditions, adopt a structure with their ionic

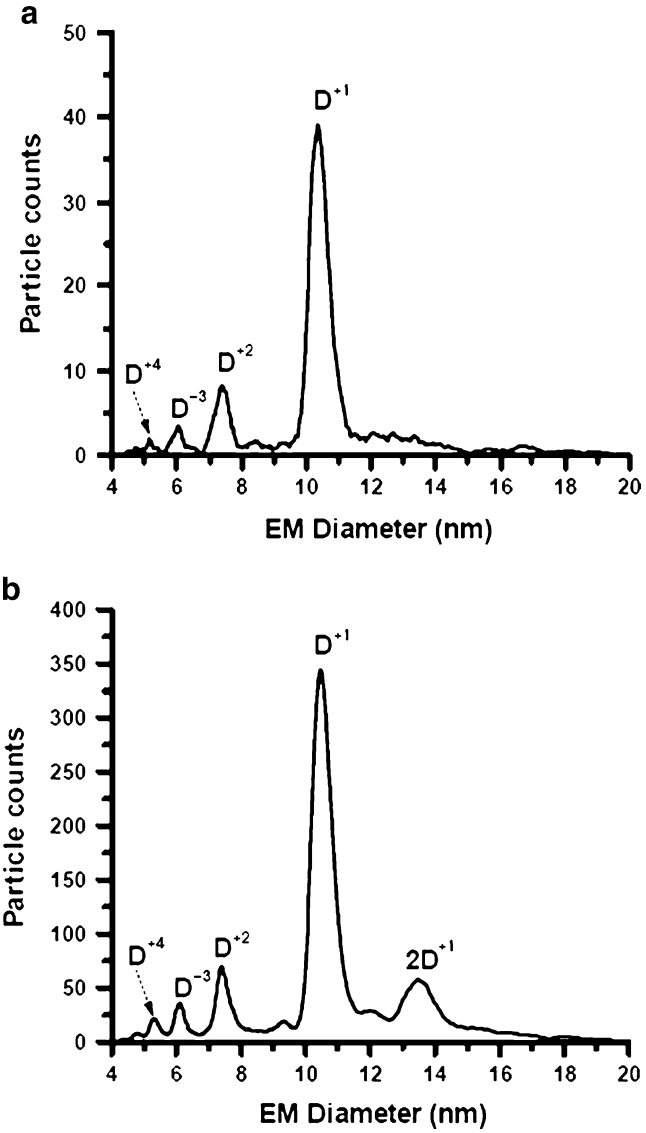

Fig. 1 NanoES-GEMMA spectra of SecA protein at 10 μg mL^{-1} (**a**) and 80 μg mL^{-1} (b). D^{+1} corresponds to the dimer biospecific non-covalent SecA complex. D^{+2}, D^{+3}, D^{+4} correspond to the doubly, triply, and quadruply charged SecA dimer, respectively. $2D^{+1}$ corresponds to the nES-induced non-specific complex of two SecA dimers

Table 1 Protein EMD, D_H, and M_r values determined using nES-GEMMA, MALLS, and QELS and their comparison

Protein analyzed	Measured	nES-GEMMA	MALLS	QELS	% Diff.[a]	Predicted M_r[b]	Other studies: references
SecA 6-901	EMD or D_H (nm)[c]	10.08±0.04	n.a.	11.0±0.5	8.4	–	–
	M_r (kDa)	196.0±2.3	210.5±13.4	n.a.	6.9 (6.3)	104.53	–
	Oligometric state[d]	Dimer	Dimer	–	–	–	Dimer: 41
	n[e]	5	16	16	–	–	–
SecA 6-834	EMD or D_H (nm)	9.87±0.01	n.a.	11.0±1.6	10.3	–	–
	M_r (kDa)	181.70±0.1	187.3±8.4	n.a.	3.0 (4.3)	94.91	–
	Oligometric state	Dimer	Dimer	–	–	–	Dimer: 57
	n	4	3	3	–	–	–
GFP-GBP-YFP	EMD or D_H (nm)	7.96±0.08	n.a.	8.8	9.5	–	–
	M_r (kDa)	95.6±2.8	91.4	n.a.	−4.6 (−4.8)	91.22	–
	Oligometric state	Monomer	Monomer	–	–	–	Monomer
	n	5	1	1	–	–	–
SecB	EMD or D_H (nm)	7.53±0.01	n.a.	8.54±1.14	11.8	–	–
	M_r (kDa)	80.9±0.1	80.6±3.5	n.a.	−0.4 (−1.5)	19.93	–
	Oligometric state	Tetramer	Tetramer	–	–	–	Tetramer: 42
	n	3	8	8	–	–	–
GBP	EMD or D_H (nm)	7.22±.013	n.a.	7.6	5.1	–	–
	M_r (kDa)	71.2±4.0	77.4	n.a.	8.0 (−3.1)	34.54	–
	Oligometric state	Dimer	Dimer	–	–	–	Monomer in reduced form: 32
	n	4	1	1	–	–	–
GBP-YFP	EMD or D_H (nm)	7.01±0.05	n.a.	8.2	14.5	–	–
	M_r (kDa)	65.2±1.4	67.0	n.a.	2.7 (−4.9)	62.13	–
	Oligometric state	Monomer	Monomer	–	–	–	Monomer
	n	4	1	1	–	–	–
CesAB+EspA	EMD or D_H (nm)	5.72±0.03	n.a.	4.9±1.2	−17	–	–
	M_r (kDa)	35.33±0.58	35.4±1.4	n.a.	0.2 (−0.7)	35.09	–
	Oligometric state	1:1 Heterodimer	1:1 Heterodimer	–	–	–	1:1 Heterodimer: 35
	n	3	6	–	–	–	–
CesAB	EMD or D_H (nm)	5.59±0.32	n.a.	5.6±0.9	0.2	–	–
	M_r (kDa)	33.3±5.6	22.7±1.6	n.a.	−46.8 (−18.8)	14.02	–
	Oligometric state	Dimer	Dimer	–	–	–	Dimer: 35
	n	6	11	3	–	–	–
YFP	EMD or D_H (nm)	5.52±0.10	n.a.	6.8	18.8	–	–
	M_r (kDa)	31.8±1.8	45.8	n.a.	30.6 (−9.6)	29.01	–
	Oligometric state	Monomer	Monomer/dimer	–	–	–	Monomer: 33, 58
	n	5	1	1	–	–	–
PpiA	EMD or D_H (nm)	4.62±0.11	n.a.	4.94±0.24	6.09	–	–
	M_r (kDa)	18.7±1.2	19.9±2.0	n.a.	5.9 (2.7)	19.21	–
	Oligometric state	Monomer	Monomer	–	–	–	Monomer: 59
	n	3	5	4	–	–	–
PspE	EMD or D_H (nm)	4.0±0.2	n.a.	n.d.	–	–	–
	M_r (kDa)	12.2±1.8	10.07±0.96	n.a.	−21.2 (−16.3)	10.49	–
	Oligometric state	Monomer	Monomer	–	–	–	Monomer: 60
	n	3	3	–	–	–	–

n.a. not applicable, *n.d.* not determined

[a] Percent difference between results from nES-GEMMA (proteins in AmAc buffer) and MALLS/QELS (proteins in Tris buffer); in parenthesis, percent difference between predicted M_r and nES-GEMMA-determined M_r

[b] Predicted M_r value obtained from the primary sequence of the protein monomer

[c] EMD and D_H referred to GEMMA and QELS measurements, respectively

[d] Main oligomeric state detected by each technique

[e] Number of replicate analyses

groups self-solvated in their interior. This results in a reduced protein volume and, thus, diameter. Protein contraction has also been suggested by Kaddis et al. [23] when comparing nES-GEMMA results with crystallographic sizing data for holo- and apo-ferritin.

Similarly, the di-SecA complex observed when analyzing the SecA 6-834 derivative (missing the carboxy-terminal C-tail of 70 residues compared to SecA 6-901) [36, 38] was determined to have an EMD of 9.87±0.01 nm compared to a D_H of 11.0 nm determined by QELS. The M_r of the non-covalent di-SecA complex, determined following the analysis of SecA 6-901 using nES-GEMMA, was calculated (Eq. 4 in ESM) to be 196 kDa. The M_r values derived from nES-GEMMA and MALLS were found to differ by 6.9%, whereas a 6.3% difference was observed between the nES-GEMMA measurement and the protein complex's predicted value. Similarly, when analyzing SecA 6-834, the M_r for di-SecA determined using nES-GEMMA and MALLS measurements differed by only 3%, whereas the nES-GEMMA value differed by only 4.3% from the complex's predicted M_r. Previous work [4, 12] using nES-GEMMA has demonstrated a mass accuracy ±1–5% for commercially available and well-characterized proteins and biomolecule complexes ranging from 8 kDa to 1 MDa.

From the analysis of these two di-SecA protein complexes, originating from SecA and SecA 6-834, which differ by 70 residues, it is observed that the nES-GEMMA and MALLS techniques can detect M_r differences corresponding to such small protein structural changes, whereas only nES-GEMMA, and not QELS, seems to detect a size difference.

We next extended our analysis to several other proteins that cover a range of sizes and oligomeric states. Table 1 contains size and M_r data for all the proteins and protein complexes analyzed in this study using all three of the compared analytical techniques. In general, it was observed that all analyzed proteins and their complexes gave predominantly similar results when using each of the techniques. Thus, determined sizes, M_r, and the predominant oligomeric states of the proteins are in general agreement between these techniques.

Even though the measured average EMD and determined M_r of some proteins (PspE, CesAB) were found to differ between the techniques, these differences are not necessarily significant because of the measurement uncertainty associated with each technique. For PspE, the predicted value of M_r 10.49 kDa is within the precision range of the GEMMA measurement, i.e., 12.2±1.8 kDa. In the case of CesAB, even though its size is in agreement between GEMMA and QELS with only a 0.2% difference (Table 1), its determined M_r values differ by more than 40%. A likely explanation for this discrepancy is that CesAB is a protein with extended natively unstructured regions (B. Kalodimos, personal communication) and the GEMMA approach used to calculate M_r from EMD assumes a spherical protein. For this natively unfolded protein, the nES-GEMMA measurements had a relative large standard deviation of 17%. This was also the only case in which GEMMA gave larger sizes than QELS.

In all other cases, EMD measurements using nES-GEMMA were on average 8.4% smaller than the protein diameters determined using QELS. It was also observed that the precision of the nES-GEMMA technique (as determined from multiple consecutive runs of the same sample, with each run lasting 60–180 s) was exceptionally good. This figure of merit is not easily determined for MALLS/QELS approaches because of the much longer time required for each SEC run and the need for column re-equilibration after each chromatographic run, in addition to the significantly larger amount of protein required for each analysis. nES-GEMMA has also demonstrated exceptional reproducibility (i.e., precision determined for runs on different days), as observed from the standard deviations reported in Table 1, determined to be in most cases better than ±0.1 nm, with the exception of CesAB with ±0.32 nm for $n=6$.

In general, it can be stated that the three analytical techniques examined here have provided complementary information in terms of protein size and relative molecular mass for various proteins and protein complexes when analyzed at considerably different concentration levels and amounts. QELS and MALLS require large amounts of protein: For a protein of 200 kDa, ~0.25–1 mg per measurement is used; for a protein of 50–80 kDa, ~0.5–1.5 mg per measurement is used; for a protein of ~10 kDa, ~1–2 mg per measurement is used. In contrast, for a single nES-GEMMA protein analysis, approximately 1.6 ng of protein is consumed; therefore, the technique seems ideally suited for the analysis of difficult to obtain protein samples. The nES-GEMMA instrumentation used can provide protein EMD ranging from 3 to 150 nm [12]. This corresponds to a calculated M_r of 8 kDa–80 MDa. MALLS has a radius of gyration lower limit of 10 nm and is capable of determining M_r within a range of 10^4–5×10^6 Da. Protein hydrodynamic diameters that can be measured by QELS range from 1 nm to a few micrometers. A summary and comparison of some of the analytical figures of merit of the three analytical techniques are presented in Table 2. Some additional technique performance characteristics, which have not been examined in this study in detail but are of significance, have also been included in Table 2 in order to allow for a more comprehensive comparison.

To place these measurements into the broader context of available state-of-the-art bioanalytical techniques, we used mass spectrometry to analyze a preparation of CesAB, identical to the one described in Table 1 as being present

Table 2 Comparison of general characteristics of the techniques used in this study for protein sizing and M_r determination

Technique characteristics	nES-GEMMA	MALLS	QELS
Sizing range (nm)	3–150	n.a.	1–1,000
Size measurement precision (nm)	0.1	n.a.	n.d.
Relative molecular mass range (kDa)	8–80,000	10–5,000	n.a.
Mass measurement accuracy (%)	1–10	0.1–1	n.a.
Measurement accuracy limitation	No commercial marker proteins >1MDa. Theoretical upper limit is 150 nm or 80 MDa	Larger particles scatter more than smaller ones. SEC separation is critical.	
Measurement bias	Assumes proteins to be spherical	Non-biased, independent of markers	
Measurement environment	Gas phase	Aqueous phase	
Capability to measure non-covalent complexes	Yes	Yes	
Buffer compatibility/main buffer	nES compatible buffers/AmAc, pH 7–8	No restrictions/Tris, pH 8.0	
Typical concentration used for analysis	1–10 μg mL^{-3}	1 mg mL^{-1}	10 mg mL^{-1}
Amount required for analysis	0.025-0.25 μg	>0.2 mg	1 mg
Amount consumed during analysis	1.6 ng	non-destructive	
Single measurement time (min)	1–4	20–40 (for SEC separation)	
Data analysis time (min)	<1	20–40	
Sample collection after analysis while maintaining functionality	Potentially yes	Yes	

n.a. not applicable, *n.d.* not determined

predominantly as a dimeric complex. This was achieved using a high-resolution and high mass accuracy LTQ-Orbitrap mass spectrometer (ESM Fig. S1). CesAB was first analyzed using the LTQ-Orbitrap under denatured conditions. Deconvoluted ES-MS spectra revealed an average relative molecular mass of 13,439.246±0.026 Da for the CesAB monomer (ESM Fig. S1a). This experimentally determined mass differs from the predicted average theoretical molecular mass by −472 Da which is due to a determined posttranslational removal of the amino-terminal Met and the carboxy-terminal Lys-Ilv-Val residues of CesAB (data not shown). Subsequently, a 10 nM CesAB solution was analyzed on the LTQ-Orbitrap mass spectrometer under native conditions (20 mM AmAc) in order to maintain the native conformation of the dimer and determine its relative molecular mass. Only a minor population of dimer (~5% that of the monomer) was detectable under these conditions with a measured average molecular mass of 26,878.341±0.030 Da (ESM Fig. S1b). Compared to the methods used here, the LTQ-Orbitrap MS analysis shows superior mass accuracy, sufficiently so as to allow for the detection of a posttranslational modification. Nevertheless, in contrast to nES-GEMMA, these measurements are generally limited to small-sized proteins in the LTQ-Orbitrap and, as seen for native CesAB, may disrupt oligomeric protein assemblies to various extents due to in-source fragmentation, vacuum disruption during the transfer from atmospheric pressure to high vacuum conditions. However, it should be stressed that state-of-the-art mass spectrometric techniques have been used to efficiently analyze non-covalent complexes following minor instrument modifications [7].

Non-covalent protein complexes analyzed by nES-GEMMA

Another important aspect of nES-GEMMA is its reported capability to preserve and detect non-covalent protein complexes [4, 8, 12, 13, 23]. This is not necessarily anticipated because of the various processes the protein complexes undergo during their transition from the aqueous to the gas phase. These processes are currently being studied extensively in order to fully evaluate and understand the technique's capability to preserve non-covalent protein complexes and their functionality and to also understand and predict the formation of potential method-specific oligomer artifacts that are unlikely to have any biological significance. This is in contrast to MALLS/QELS measurements which are made in aqueous solution and thus the proteins can be easily kept in their native state and their functionality maintained provided an appropriate buffer is used. Thus, biospecific non-covalent protein complexes remain intact during these measurements and biochemical activity can be readily demonstrated at the end of such a determination in the fractions that are collected following their SEC separation.

The nES-GEMMA measurements made for protein complexes in this study show that non-covalent protein interactions are not disrupted (see oligomeric states in Table 1). In fact, our data clearly agree with previous studies [4, 8, 13, 14, 39, 40] that have reported on the existence of non-covalent protein complexes for the various proteins analyzed here. SecA is detected mainly as a dimer [41], the state that is seen in various preparations, whereas SecB is observed mainly as a tetramer, which again is what is expected for the buffer that is used (20 mM AmAc at pH 6.9) [42]. CesAB, expected to be dimeric [35], is detected by nES-GEMMA as such. GBP is a covalent dimer formed through an intermolecular disulfide and is used here as an internal control. In fact, nES-GEMMA data confirmed GBP to be a dimer, which is in agreement with its MALLS/QELS measurements. All other proteins analyzed here are known to exist as monomers.

Following the analysis of the homo-oligomers, we went on to analyze solutions containing two different proteins that are expected to form biospecific non-covalent interactions. More specifically, we analyzed a solution containing proteins that are expected to form a complex consisting of a chaperone (CesAB) and its secretory protein substrate (EspA) that are involved in the bacterial type III secretion pathway of enteropathogenic *E. coli* bacteria [43, 44]. Crystallographic data demonstrated that CesAB forms a one-to-one stoichiometric complex with EspA [35]. The EMD of 5.72 nm determined using GEMMA and its calculated M_r of 35.3 kDa are in good agreement with the values of 4.9±1.2 nm and 35.4 kDa, respectively, derived from MALLS and QELS measurements, respectively. This is another example of the capability of nES-GEMMA to maintain non-covalent interactions, specifically between different proteins.

However, it remains to be examined in nES-GEMMA how these protein complexes behave during their gas phase "journey" through the IMS, which takes place in atmospheric pressure, i.e., do they maintain their functionality? Allmaier et al. [13] have already mentioned the collection of intact tobacco mosaic virus using an electrostatic particle sampler after GEMMA analysis. Thus, the collection of proteins and protein complexes and the examination of their biological activity will be of great interest as specific protein quaternary states can be correlated to specific functions.

nES-induced protein oligomers

In previous publications [4, 8, 12, 22, 23], the nES-GEMMA technique has been reported to analyze protein concentrations ranging from 1 to about 10 μg protein per milliliter. In some of these studies, it was implied that at higher concentrations, non-specific oligomers form as a result of the nES-GEMMA process. However, to date, this occurrence has received limited systematic study [45, 46]. To investigate this further, a nES-GEMMA electropherogram for a solution containing 80 μg SecA protein per milliliter (Fig. 1b) was recorded, in which case an extra peak, compared to the one resulting from the analysis of the 10 μg mL^{-1} protein solution (Fig. 1a), was detected at 13.2 nm. Based on the determined and predicted M_r of di-SecA (i.e., 197 and 204.02 kDa, respectively), the extra peak is assigned to correspond to a SecA tetramer as its determined M_r is 431 kDa. The observed SecA tetramer is considered to form as a result of non-specific interactions between two di-SecA complexes. This tetrameric SecA species is most likely generated as a result of the nES-GEMMA process since it has neither been identified during chromatographic separation of SecA [41] nor seen in crystal or cryo-electron microscopy structures [31] and is therefore not likely to be of biological relevance. In fact, its formation is in accordance with the reported tendency of nES to induce the formation of non-specific oligomers when spraying solutions containing high concentrations of proteins [4]. As such, we consider the source of these non-specific oligomers to be the nES process itself and thus refer to them as "nES-induced" oligomers [4].

The occurrence of such nES-induced oligomers is not necessarily a limitation when using nES-GEMMA to study the existence of non-covalent protein complexes. This is because such oligomers can be readily identified as they only occur at high concentrations (typically >20 μg mL^{-1}), and they are integer multimers of the most abundant aqueous phase protein species, i.e., in the case of SecA which occurs mainly as a dimer we observe nES-induced tetramers, whereas trimers seem to be absent. In case of dilution of such highly concentrated solutions, non-specific oligomers will disappear more readily whereas biospecific oligomers will remain detected.

To improve our understanding of this occurrence, we analyzed the SecB tetramer which gives nES-induced oligomers as octamers and dodecamers when analyzed in concentrated solutions (Fig. 2a). As in the case of SecA (Fig. 1b), the formation of nES-induced oligomers is mainly concentration-dependent. Thus, it is evident that low protein concentrations, usually <10 μg mL^{-1}, are preferable in order to reduce or eliminate the possibility of the occurrence of such non-specific associations (Fig. 2a). So far, the majority of nES-GEMMA publications reporting the analysis of proteins and protein complexes have analyzed solutions containing low protein concentrations, typically from 1 to 10 μg mL^{-1}. In Fig. 2b, we present an example highlighting the distinct behavior of biospecific and nES-induced protein interactions, thus allowing for their potential identification. When SecB is analyzed at a concentration of 10 μg mL^{-1}, a concentration at which non-

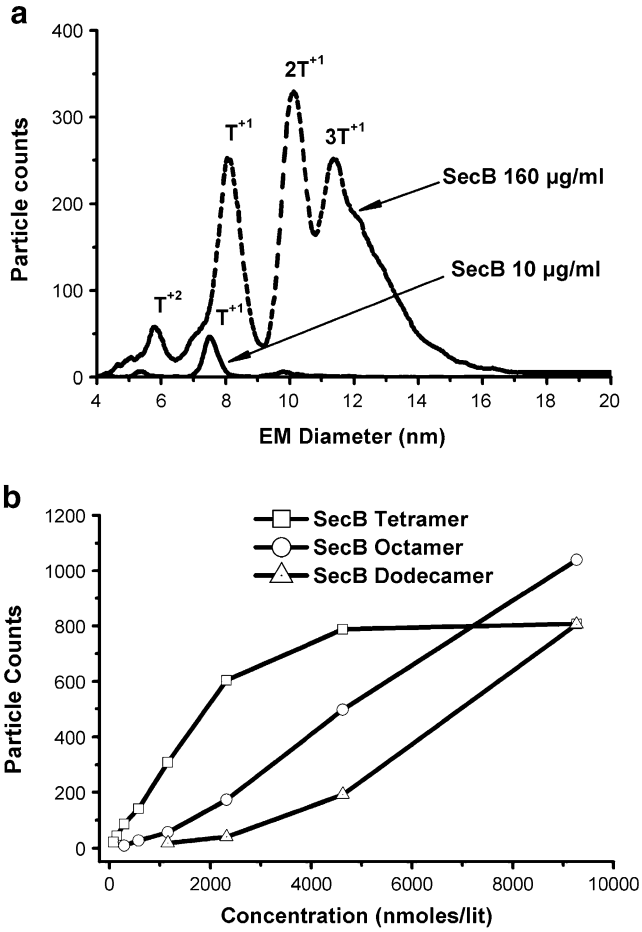

Fig. 2 Overlaid nES-GEMMA spectra of SecB at two different concentrations (10 and 80 µg mL^{-1}) (**a**), and particle counts of the different SecB oligomers (tetramer, octamer, twelvemer) vs. SecB concentration (**b**). T^{+1} corresponds to the tetrameric biospecific non-covalent SecB complex. T^{+2} corresponds to the double charged SecB tetramer. $2T^{+1}$, $3T^{+1}$ correspond to the nES-induced non-specific complex of two and three SecB tetramers, respectively

specific interactions are not expected to occur to any significant extent, only the biologically relevant SecB tetramer is observed. Increasing the concentration 16-fold yields extensive non-specific interactions, as observed from the formation of nES-induced oligomers (Fig. 2), i.e., 8-mer and 12-mers, with relative intensities that decrease with oligomer size.

Analyzing a protein over a wide concentration range reveals a pattern that helps distinguish between the occurrence of native and nES-induced protein associations (Fig. 2b). Within the wide concentration range analyzed, it is observed that the intensity of the main or native species (non-covalent SecB tetramer) increases linearly until a plateau is reached. Thus, the response curve for the major species consists of an initial linear region, having a steep slope as a result of the increasing protein concentration in the analyzed solutions. The response slope subsequently levels off as a result of what we believe to be the participation of the main species (i.e., SecB tetramer) in the formation of nES-induced oligomers. After analyzing a series of proteins and protein complexes, we have found the concentration at which this abrupt slope transition occurs to be protein-dependent. The response curve for the first suspected nES-induced oligomer peak, i.e., octamer in this case, also consists of an initial linear region with a shallow slope, indicating its possible presence in solution at low concentrations or if the slope is zero, its complete absence from solution. Subsequently, an abrupt slope increase for the SecB octamer indicates an additional source of the complex, which we consider to be from the nES process. It is important to stress that the formation of nES-induced oligomers is not just concentration-driven but also protein-dependent (ESM Fig. S2). We anticipate that the presence of patches of different ionizable or hydrophobic residues on the surface of a protein might influence protein–protein aggregation in the nES droplets prior to their gas-phase introduction.

Another parameter that seems to significantly affect the extent of nES-induced oligomer formation and may correlate with protein surface properties is buffer concentration. An example of this is shown in Fig. 3a where it is observed that when increasing the concentration of the AmAc buffer from 5 to 80 mM the nES-induced SecA tetramer at 13 nm is no longer observed, whereas the main di-SecA species undergoes a minor intensity decrease. A similar trend is observed for the analysis of elevated concentrations of transferrin (Fig. 3b). In which case, the intensity of transferrin oligomers ($2M^+$ and $3M^+$) are significantly reduced when using 80 mM AmAc concentration, whereas the intensity of the main transferrin peak corresponding to M^+ increases. The reason for this occurrence is not clear; however, it has been shown in a previous study [47] that Coulomb explosions on electrosprayed droplets are eliminated when electrospraying high conductivity solutions. This would make it unlikely for the proposed charge residue model (CRM) of Dole et al. [48] to be occurring, even though it is the mechanism believed to be responsible for the formation of singly charged macromolecules [6, 49, 50] and ions of globular proteins [51]. If this is the case, an alternative mechanism, such as the ion evaporation model [52, 53] or a variation of the CRM, would be responsible for the formation of gas-phase ions and the observed reduction or elimination of the nES-induced oligomers. An alternative explanation stems from the fact that upon electrospraying lower conductivity solutions [54] or lower AmAc [46] concentrations in the cone-jet mode, the resulting droplet sizes are larger, which in turn increases the probability that a droplet will contain more than one protein molecule. Droplets containing more than one protein molecule will result in oligomer formation upon droplet drying according to the CRM. Furthermore, it

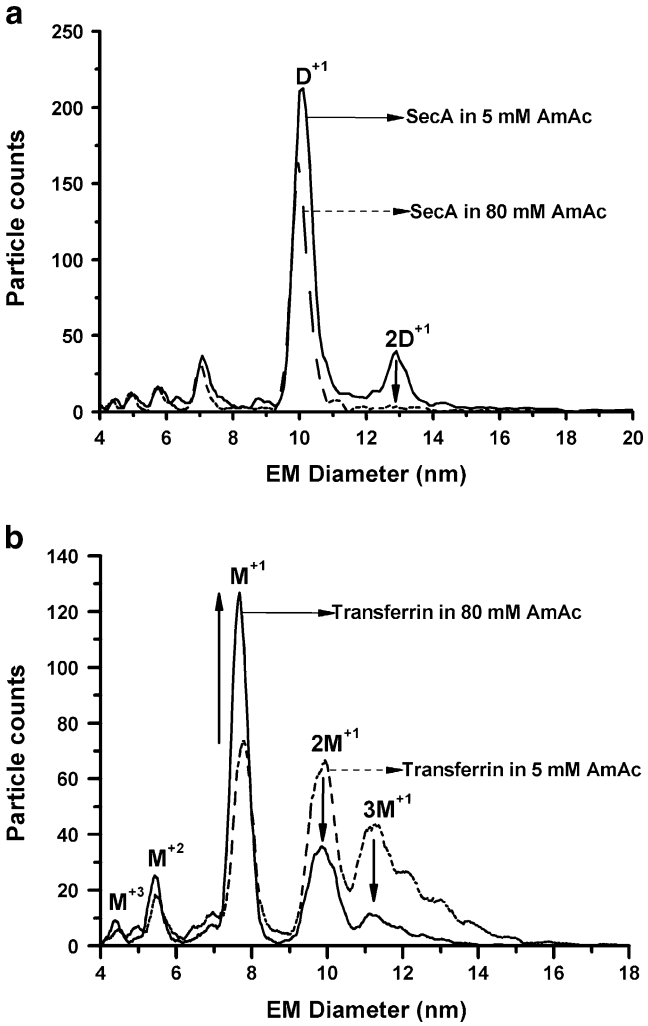

Fig. 3 NanoES-GEMMA spectra of SecA (20 μg mL^{-1}) (**a**) and transferrin (20 μg mL^{-1}) (**b**), each obtained at 5 and 80 mM AmAc concentration. The *vertical arrows* indicate the reduction of nES-induced oligomer intensity, observed when using higher buffer concentration

is also possible that increased buffer concentration may contribute toward the weakening of electrostatic interactions between the subunits, thus limiting oligomerization.

Analytical figures of merit for nES-GEMMA

Typically, when using nES-GEMMA, a 25 μL protein solution with a concentration of 1–10 μg mL^{-1} (≈10 nmol L^{-1}) is required for analysis. Thus, for every run, only 0.025–0.25 μg of protein is needed when using a 1-mL Eppendorf tube to hold the sample solution. However, it should be stressed that a much smaller amount of protein is actually consumed, i.e., approximately 1.6 ng of protein is consumed as the analysis takes place at a flow rate of approximately 70 nL min^{-1} (Table 2). MALLS/QELS techniques require a much larger amount of protein, typically ranging from 0.25 to 2 mg. Another differentiating feature of nES-GEMMA is that protein separation and size determination takes place simultaneously in the ion mobility spectrometer. However, in the MALLS/QELS technique, results are optimal when size exclusion chromatography is used for the protein separation followed by size and mass determination from the MALLS/QELS detectors. Good SEC separation of chromatographic peaks is important for the accurate measurement by MALLS/QELS in the case of protein mixtures. The resolving power of nES-GEMMA system is ≈5–7 full width at half-maximum [12], which is similar to the reported values for SEC.

A unique feature of the nES-GEMMA technique that remains to be further explored is that it "freezes" chemical bimolecular equilibria between protein complexes during the nES process and subsequently separates them using GEMMA. However, even though this is a significant feature of nES-GEMMA, the technique itself does not seem to be ideal for quantitatively monitoring real-time dynamic processes in aqueous environments, such as protein oligomerization induced by the presence of particular ligands and homo-oligomerization induced by high protein protomer or subunit concentrations. This is mainly because of the species-dependent sensitivities exhibited by nES as well as the limited working concentration range for avoiding nES-induced oligomers. MALLS/QELS would be better tools for studying such processes. However, given the nanomolar sensitivity of the nES-GEMMA technique, we expect protein systems with dissociation constants in the high nanomolar to micromolar range to be suitable for such studies. At this concentration range, current MALLS/QELS detectors are either below or at their detection limit.

NanoES-GEMMA is a "buffer-restricted" technique because of the nES source restrictions. The buffer most commonly used is 20 mM AmAc at pH 7–8. In this work, the proteins were dialyzed in this buffer. To test whether the buffer system affects protein function, the ATPase activity of SecA was measured and shown to be indistinguishable from that in other buffer systems (ESM Fig. S3). Other aqueous buffer solutions may also be used, such as 0.05% trifluoracetic acid, 20 mM nitric acid, 20 mM hydrochloric acid, triethyl amine, and 20 mM acetic acid, as specified by the nES-GEMMA manufacturer (TSI Inc.). Also, in the present study, additional buffers such as ammonium bicarbonate and ammonium acetate/ammonium formate 1:1 (*v*/*v*) mixture were tested and considered compatible (data not shown). In general, volatile buffers with conductivities >0.2 S m^{-1} are recommended for use [55]. Any non-volatile salts, surfactants, or other non-volatile solutes should be removed (dialysis, ultrafiltration, etc.) because they tend to form clusters during the nES process [56], which, depending on their size and concentration, may

cause interference. MALLS/QELS does not suffer from these limitations and runs with a variety of protein compatible buffers. Apart from the buffering species, high (mM) concentrations of other additives may not be suitable for use with nES-GEMMA as they contribute to high background signals. These include small molecule ligands frequently studied in biological systems (e.g., nucleotides, peptides, etc.) or additives for structural analysis (e.g., trifluoroethanol) or crowding agents (e.g., glycerol).

The time required for the complete analysis of a protein sample (2–4 min) by nES-GEMMA makes this technique appropriate for high-throughput protein analysis. It takes approximately 110 s for the sample to fill the nanoelectrospray capillary when the solution uptake flow rate is 70 nL min^{-1}, which is achieved using an external uptake pressure of 3.8 psi. The resulting charged proteins travel through the ion mobility spectrometer and the CPC detector at a 6- to 15-L min^{-1} gas flow rate in approximately 0.4 and 3.27 s (2.72 s in the transfer tube taking them from the DMA to the CPC, plus 0.55 s in the detector), respectively. Note that overall analysis times may vary as they depend on capillary flow characteristics and other system settings such as gas flow rate and scan time. The scan time is usually adjusted to 60–135 s in order to achieve improved signal-to-noise ratios. Also, data analysis is typically rapid, requiring <1 min for the analysis of each electropherogram. In contrast, MALLS/QELS requires 20–40 min per run and 20–40 min per software analysis for each run (Table 2). In this respect, it seems that nES-GEMMA is significantly faster than MALLS/QELS.

Conclusions

In comparison with the more established MALLS and QELS techniques, nES-GEMMA offers several complementary advantages. It requires considerably less amount of material and time per sample analysis. Because of short analysis times, nES-GEMMA is better suited for larger sample set screening, whereas size and relative molecular mass measurements are similar between the compared methods. However, GEMMA seems to systematically "shrink" protein size by approximately 10% compared to the hydrodynamic diameter derived by QELS. Some of the technique's disadvantages include that it cannot be used to measure high concentration levels because of the potential occurrence of nES-induced oligomers and is prone to interference by high concentrations of small molecule ligands and salts. However, this disadvantage can be alleviated in some cases by diluting the protein solution. Also, nES-GEMMA is not compatible with all the buffers commonly used with MALLS and QELS. Overall, nES-GEMMA shows promise as a high-throughput proteomics/protein structure tool.

Acknowledgments We are grateful to Dr. M. Papanastasiou for discussions, to Dr. G. Gouridis for help with the MALLS instrument, and to members of the Economou laboratory for protein samples. The research leading to these results has received funding from the European Commission (EC) through the funding of a Marie Curie Excellence Grant MEXT-CT-2003-002788 (to S.A.P.) and from the EC's Sixth Framework Programme agreement no. LSHC-CT-2006-037834 "Streptomics" (to A.E.), the Greek General Secretariat of Research and the European Regional Development Fund (PENED03ED623) (to A.E.), and from the European Community's Sixth Framework Programme agreement 031867–Integrated Project P. Cezanne (to A.E.). The proteomics facility of the IMBB was established through the European Community's Seventh Framework Programme agreement 229823 Capacities-FP7-REGPOT-2008-1/project "ProFI". M.F.S. is an Onassis foundation pre-doctoral fellow. Also, E.A.K. thanks the Greek Ministry of Education, Lifelong Learning and Religious Affairs for funding an Hrakleitos II PhD studentship.

References

1. Robinson CV, Sali A, Baumeister W (2007) The molecular sociology of the cell. Nature 450(7172):973–982
2. Devos D, Russell RB (2007) A more complete, complexed and structured interactome. Curr Opin Struct Biol 17(3):370–377
3. Kocher T, Superti-Furga G (2007) Mass spectrometry-based functional proteomics: from molecular machines to protein networks. Nat Methods 4(10):807–815
4. Bacher G, Szymanski WW, Kaufman SL, Zollner P, Blaas D, Allmaier G (2001) Charge-reduced nano electrospray ionization combined with differential mobility analysis of peptides, proteins, glycoproteins, noncovalent protein complexes and viruses. J Mass Spectrom 36(9):1038–1052
5. de la Mora JF, Ude S, Thomson BA (2006) The potential of differential mobility analysis coupled to MS for the study of very large singly and multiply charged proteins and protein complexes in the gas phase. Biotechnol J 1(9):988–997
6. Kaufman SL, Skogen JW, Dorman FD, Zarrin F, Lewis KC (1996) Macromolecule analysis based on electrophoretic mobility in air: globular proteins. Anal Chem 68(11):1895–1904
7. Sharon M, Robinson CV (2007) The role of mass spectrometry in structure elucidation of dynamic protein complexes. Annu Rev Biochem 76:167–193
8. Loo JA (1997) Studying noncovalent protein complexes by electrospray ionization mass spectrometry. Mass Spectrom Rev 16(1):1–23
9. Kaufman SL, Kuchumov AR, Kazakevich M, Vinogradov SN (1998) Analysis of a 3.6-MDa hexagonal bilayer hemoglobin from *Lumbricus terrestris* using a gas-phase electrophoretic mobility molecular analyzer. Anal Biochem 259(2):195–202
10. Benesch JL, Robinson CV (2006) Mass spectrometry of macromolecular assemblies: preservation and dissociation. Curr Opin Struct Biol 16(2):245–251
11. Ruotolo BT, Robinson CV (2006) Aspects of native proteins are retained in vacuum. Curr Opin Chem Biol 10(5):402–408
12. Kaddis CS, Loo JA (2007) Native protein MS and ion mobility: large flying proteins with ESI. Anal Chem 79(5):1778–1784
13. Allmaier G, Laschober C, Szymanski WW (2008) Nano ES GEMMA and PDMA, new tools for the analysis of nanobioparticles–protein complexes, lipoparticles, and viruses. J Am Soc Mass Spectrom 19(8):1062–1068
14. Laschober C, Wruss J, Blaas D, Szymanski WW, Allmaier G (2008) Gas-phase electrophoretic molecular mobility analysis of size and stoichiometry of complexes of a common cold virus with

antibody and soluble receptor molecules. Anal Chem 80(6):2261–2264
15. Scalf M (1999) Controlling charge states of large ions. Science 283(5410):2105
16. Reischl GP, Makela JM, Karch R, Necid J (1996) Bipolar charging of ultrafine particles in the size range below 10 nm. J Aerosol Sci 27(6):931–949
17. Fuchs NA (1963) On the stationary charge distribution on aerosol particles in bipolar ionic atmosphere. Pure Appl Geophys 56 (1):185–193
18. Agarwal JK, Sem GJ (1980) Continuous-flow, single-particle-counting condensation nucleus counter. J Aerosol Sci 11(4):343
19. Kesten J, Reineking A, Porstendorfer J (1991) Calibration of a TSI-model-3025 ultrafine condensation particle counter. Aerosol sci tech 15(2):107–111
20. Carazzone C, Raml R, Pergantis SA (2008) Nanoelectrospray ion mobility spectrometry online with inductively coupled plasma–mass spectrometry for sizing large proteins, DNA, and nanoparticles. Anal Chem 80(15):5812–5818
21. Thomas JJ, Bothner B, Traina J, Benner WH, Siuzdak G (2004) Electrospray ion mobility spectrometry of intact viruses. Spectrosc Int J 18(1):31–36
22. Loo JA, Berhane B, Kaddis CS, Wooding KM, Xie Y, Kaufman SL, Chernushevich IV (2005) Electrospray ionization mass spectrometry and ion mobility analysis of the 20S proteasome complex. J Am Soc Mass Spectrom 16(7):998–1008
23. Kaddis CS, Lomeli SH, Yin S, Berhane B, Apostol MI, Kickhoefer VA, Rome LH, Loo JA (2007) Sizing large proteins and protein complexes by electrospray ionization mass spectrometry and ion mobility. J Am Soc Mass Spectrom 18(7):1206–1216
24. Hogan CJ Jr, Kettleson EM, Ramaswami B, Chen DR, Biswas P (2006) Charge reduced electrospray size spectrometry of mega- and gigadalton complexes: whole viruses and virus fragments. Anal Chem 78(3):844–852
25. Wick CH, McCubbin PE (1999) Characterization of purified MS2 bacteriophage by the physical counting methodology used in the integrated virus detection system (IVDS). Toxicol methods 9 (4):245–252
26. Muller R, Laschober C, Szymanski WW, Allmaier G (2007) Determination of molecular weight, particle size, and density of high number generation PAMAM dendrimers using MALDI-TOF-MS and nES-GEMMA. Macromolecules 40(15):5599–5605
27. Saucy DA, Ude S, Lenggoro IW, de la Mora JF (2004) Mass analysis of water-soluble polymers by mobility measurement of charge-reduced ions generated by electrosprays. Anal Chem 76 (4):1045–1053
28. Poderycki MJ, Kickhoefer VA, Kaddis CS, Raval-Fernandes S, Johansson E, Zink JI, Loo JA, Rome LH (2006) The vault exterior shell is a dynamic structure that allows incorporation of vault-associated proteins into its interior. Biochemistry 45(39):12184–12193
29. Karamanou S, Vrontou E, Sianidis G, Baud C, Roos T, Kuhn A, Politou AS, Economou A (1999) A molecular switch in SecA protein couples ATP hydrolysis to protein translocation. Mol Microbiol 34(5):1133–1145
30. Schenkman L, Koukaki M, Karamanou S, Economou A. The P. CÉZANNE Project: Innovative approaches to continuous glucose monitoring. Conference Proceedings of the IEEE Engineering in Medicine and Biology Society, Tel Aviv, 22–26 Aug. 2007, Tel Aviv 2007, pp 6060–6063
31. Sardis MF, Economou A (2010) SecA: a tale of two protomers. Mol Microbiol 76(5):1070–1081
32. Tian Y, Cuneo MJ, Changela A, Hocker B, Beese LS, Hellinga HW (2007) Structure-based design of robust glucose biosensors using a *Thermotoga maritima* periplasmic glucose-binding protein. Protein Sci 16(10):2240–2250
33. Wachter RM, Elsliger MA, Kallio K, Hanson GT, Remington SJ (1998) Structural basis of spectral shifts in the yellow-emission variants of green fluorescent protein. Structure 6(10):1267–1277
34. Liu J, Walsh CT (1990) Peptidyl-prolyl *cis-trans*-isomerase from Escherichia coli: a periplasmic homolog of cyclophilin that is not inhibited by cyclosporin A. Proc Natl Acad Sci USA 87 (11):4028–4032
35. Yip CK, Finlay BB, Strynadka NC (2005) Structural characterization of a type III secretion system filament protein in complex with its chaperone. Nat Struct Mol Biol 12(1):75–81
36. Gelis I, Bonvin AM, Keramisanou D, Koukaki M, Gouridis G, Karamanou S, Economou A, Kalodimos CG (2007) Structural basis for signal-sequence recognition by the translocase motor SecA as determined by NMR. Cell 131(4):756–769
37. Wyttenbach T, Bowers MT (2009) Hydration of biomolecules. Chem phys lett 480(1–3):1–16
38. Sianidis G, Karamanou S, Vrontou E, Boulias K, Repanas K, Kyrpides N, Politou AS, Economou A (2001) Cross-talk between catalytic and regulatory elements in a DEAD motor domain is essential for SecA function. EMBO J 20(5):961–70
39. Heck AJ, Van Den Heuvel RH (2004) Investigation of intact protein complexes by mass spectrometry. Mass Spectrom Rev 23 (5):368–389
40. McKay AR, Ruotolo BT, Ilag LL, Robinson CV (2006) Mass measurements of increased accuracy resolve heterogeneous populations of intact ribosomes. J Am Chem Soc 128 (35):11433–11442
41. Woodbury RL, Hardy SJ, Randall LL (2002) Complex behavior in solution of homodimeric SecA. Protein Sci 11(4):875–882
42. Xu Z, Knafels JD, Yoshino K (2000) Crystal structure of the bacterial protein export chaperone secB. Nat Struct Biol 7 (12):1172–1177
43. Goosney DL, Gruenheid S, Finlay BB (2000) Gut feelings: enteropathogenic *E. coli* (EPEC) interactions with the host. Annu Rev Cell Dev Biol 16:173–189
44. Spears KJ, Roe AJ, Gally DL (2006) A comparison of enteropathogenic and enterohaemorrhagic *Escherichia coli* pathogenesis. FEMS Microbiol Lett 255(2):187–202
45. Kemptner J, Marchetti-Deschmann M, Siekmann J, Turecek PL, Schwarz HP, Allmaier G (2010) GEMMA and MALDI-TOF MS of reactive PEGs for pharmaceutical applications. J Pharm Biomed Anal 52(4):432–437
46. Pease LF 3rd, Elliott JT, Tsai DH, Zachariah MR, Tarlov MJ (2008) Determination of protein aggregation with differential mobility analysis: application to IgG antibody. Biotechnol Bioeng 101(6):1214–1222
47. Gamero-Castano M, de la Mora JF (2000) Mechanisms of electrospray ionization of singly and multiply charged salt clusters. Anal Chim Acta 406(1):67–91
48. Dole M, Mack LL, Hines RL, Mobley RC, Ferguson LD, Alice MB (1968) Molecular beams of macroions. J Chem Phys 49:2240–2249
49. Mouradian S, Skogen JW, Dorman FD, Zarrin F, Kaufman SL, Smith LM (1997) DNA analysis using an electrospray scanning mobility particle sizer. Anal Chem 69(5):919–925
50. Kaufman SL (1998) Analysis of biomolecules using electrospray and nanoparticle methods: the gas-phase electrophoretic mobility molecular analyzer (GEMMA). J Aerosol Sci 29(5–6):537–552
51. de la Mora JF (2000) Electrospray ionization of large multiply charged species proceeds via Dole's charged residue mechanism. Anal Chim Acta 406(1):93–104
52. Iribarne JV, Thomson BA (1976) Evaporation of small ions from charged droplets. J Chem Phys 64(6):2287–2294
53. Thomson BA, Iribarne JV, Dziedzic PJ (1982) Liquid ion evaporation/mass spectrometry/mass spectrometry for the detection of polar and labile molecules. Anal Chem 54(13):2219–2224

54. Chen DR, Pui DYH (1997) Experimental investigation of scaling laws for electrospraying: dielectric constant effect. Aerosol sci tech 27(3):367–380
55. TSI Inc. (2006) Operation and service manual of macroion mobility spectrometer. P/N 1930110, RevA ed.
56. Juraschek R, Dulcks T, Karas M (1999) Nanoelectrospray—more than just a minimized-flow electrospray ionization source. J Am Soc Mass Spectrom 10(4):300–308
57. Karamanou S, Sianidis G, Gouridis G, Pozidis C, Papanikolau Y, Papanikou E, Economou A (2005) *Escherichia coli* SecA truncated at its termini is functional and dimeric. FEBS Lett 579(5):1267–1271
58. Zacharias DA, Violin JD, Newton AC, Tsien RY (2002) Partitioning of lipid-modified monomeric GFPs into membrane microdomains of live cells. Science 296(5569):913–916
59. Clubb RT, Ferguson SB, Walsh CT, Wagner G (1994) Three-dimensional solution structure of *Escherichia coli* periplasmic cyclophilin. Biochemistry 33(10):2761–2772
60. Li H, Yang F, Kang X, Xia B, Jin C (2008) Solution structures and backbone dynamics of *Escherichia coli* rhodanese PspE in its sulfur-free and persulfide-intermediate forms: implications for the catalytic mechanism of rhodanese. Biochemistry 47(15):4377–4385